Molecular Crystals and Liquid Crystals

ISSN: 1542-1406 (Print) 1563-5287 (Online) Journal homepage: http://www.tandfonline.com/loi/gmcl20

Photo-alignment Property of Azobenzene-containing Polyimide Films Swollen by Alkyl-amine

Kenji Sakamoto, Kiyoaki Usami & Kazushi Miki

To cite this article: Kenji Sakamoto, Kiyoaki Usami & Kazushi Miki (2015) Photo-alignment Property of Azobenzene-containing Polyimide Films Swollen by Alkyl-amine, Molecular Crystals and Liquid Crystals, 611:1, 153-159, DOI: 10.1080/15421406.2015.1030213

To link to this article: http://dx.doi.org/10.1080/15421406.2015.1030213

Published online: 06 Jul 2015.

Mole. Cryst. Liq. Cryst., Vol. 611: pp. 153–159, 2015

ISSN: 1542-1406 print/1563-5287 online
DOI: 10.1080/15421406.2015.1030213

Photo-alignment Property of Azobenzene-containing Polyimide Films Swollen by Alkyl-amine

KENJI SAKAMOTO,[1,*] KIYOAKI USAMI,[2] AND KAZUSHI MIKI[1]

[1]Polymer Materials Unit, National Institute for Materials Science (NIMS) Namiki, Tsukuba, Ibaraki, Japan
[2]Department of Information Systems Engineering, Osaka Sangyo University, Nakagaito, Daito-shi, Osaka, Japan

Photo-alignment efficiency of polyimide containing azobenzene in the backbone structure (Azo-PI) is significantly enhanced by exposing the precursor (polyamic acid: Azo-PAA) film to alkyl-amine vapor prior to photo-alignment. In this study, we have investigated the relationships between the alkyl-amine vapor treatment time, the swelling ratio of Azo-PAA films, and the photo-induced in-plane anisotropy. We found that: the Azo-PAA film swells on exposure to alkyl-amine vapor, and the swelling finally saturates; and the photo-induced in-plane anisotropy is correlated very closely with the swelling ratio. In addition, we pointed out the importance of the process order of alkyl-amine vapor treatment and photo-alignment.

Keywords Photo-alignment; azobenzene; polyimide; alkyl-amine; swelling; photoisomerization

Introduction

Establishment of surface-induced alignment methods of liquid crystals (LCs) that can replace the conventional mechanical rubbing technique is a key issue for improving the quality and performance of LC displays (LCDs). This is because the rubbing technique has serious disadvantages, such as creation of dust particles and scratches, generation of electrostatic charge, and poor uniformity, associated with the mechanical contact between the rubbing cloth and the alignment layer surface. Among various noncontact alignment methods proposed so far [1–10], photo-alignment [11] is the most promising alternative, because of its potential capability for two-dimensional alignment patterning. The patterning capability is useful for fabricating LCDs with a large viewing angle [12], for realizing multistable in-plane LC alignment over a large area [13]. In addition, photo-alignment is suitable for the mass production, because of no need of vacuum environment. In 2010, Sharp Corp.

*Address correspondence to Kenji Sakamoto, Polymer Materials Unit, National Institute for Materials Science (NIMS), 1-1 Namiki, Tsukuba, Ibaraki 305-0044, Japan. E-mail: SAKAMOTO.Kenji@nims.go.jp

Color versions of one or more of the figures in the article can be found online at www.tandfonline.com/gmcl.

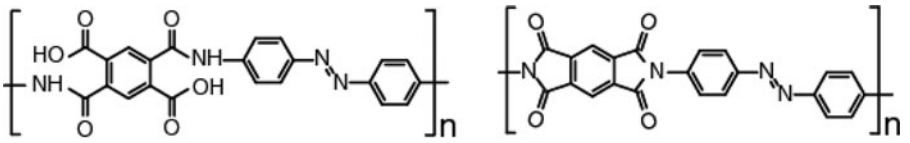

Figure 1. Molecular Structures of Azo-PAA and Azo-PI used in this study.

first adopted a photo-alignment method in the commercial product line of multi-domain vertical alignment mode LCDs.

Among a variety of photo-alignment methods, we are focusing on a method originally proposed by Park et al. [14], which is based on the photo-isomerization reaction of polyamic acid containing azobenzene in the backbone structure (Azo-PAA). In the conventional fabrication process, photo-alignment is carried out on the Azo-PAA film, and subsequently the film is thermally converted into polyimide (Azo-PI). Since the photo-responsibility disappears after conversion [15], the resultant alignment layer shows high optical stability along with the inherent high thermal and chemical stability of polyimide. In addition, we already confirmed that the Azo-PI photo-alignment layers with in-plane anisotropy larger than that induced by rubbing can be obtained [16], that a high dark-level state of LC cells can be realized by using such highly-oriented photo-alignment layers [17], and also that the azimuthal anchoring energy coefficient of the photo-alignment layers is comparable to or larger than that of conventional rubbed polyimide alignment layers [18].

Recently, we succeeded in significantly enhancing the photo-alignment efficiency of Azo-PI backbone structures by exposing the Azo-PAA film to alkyl-amine vapor prior to photo-alignment [19]. This enhancement arises from efficient photo-induced rotation of the Azo-PAA backbone structures in the film swollen by absorbing alkyl-amine molecules. Most of the alkyl-amines in the swollen film desorb during thermal imidization. In this study, we have investigated the relationships between the alkyl-amine vapor treatment time, the swelling degree of the Azo-PAA film, and the photo-induced in-plane anisotropy. From these relationships, we found that the Azo-PAA film swells on exposure to alkyl-amine vapor, and the swelling finally saturates. The photo-induced in-plane anisotropy of the Azo-PAA and Azo-PI films is correlated very closely with the swelling ratio of the Azo-PAA films. From this result, we also found that the photo-induced rotation of the Azo-PAA backbone structure becomes easier with increasing degree of swelling. Finally, we pointed out that the process order of alkyl-amine vapor treatment and photo-alignment is important for the realization of photo-alignment efficiency enhancement.

Experimental

In this study we used Azo-PAA with the polystyrene equivalent weight average molecular weight (M_w) of 24600 and the polydispersity of 2.9. The molecular structure is shown in Fig. 1, together with that of the corresponding Azo-PI. The Azo-PAA films were formed on quartz glass substrates ($20 \times 20 \times 1^t$ mm^3) by spin-coating with a filtered solution of Azo-PAA (1.6 wt.%) in N-methyl-2-pyrrolidone at 3000 rpm for 60 s, and then soft-baked at 80°C for 2 min in air to remove the residual solvent. Then, the Azo-PAA films were exposed to octadecylamine (ODA) vapor for different treatment times. The details of this treatment was described in our previous paper [19]. Then, photo-alignment was performed using a 500 W

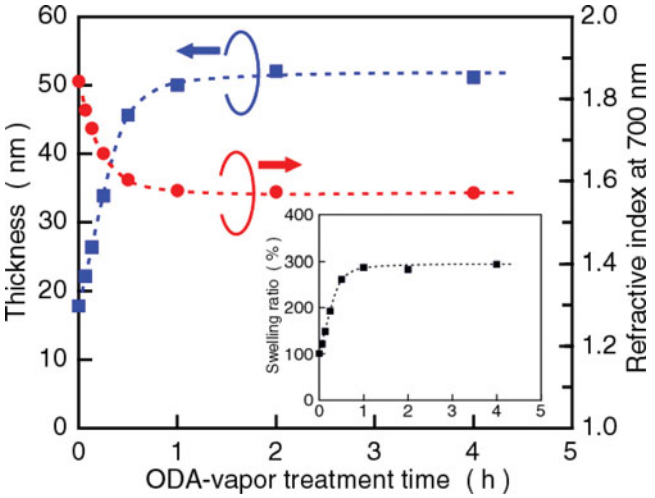

Figure 2. Thickness and refractive index at 700 nm of the Azo-PAA films exposed to ODA vapor at 80°C with different treatment times. The inset shows the ODA vapor treatment time dependence of the swelling ratio. The broken curves are guides to the eye.

deep UV lamp (Ushio Inc. UXM-501MD) as the light source. The wavelength was selected with a band-pass filter of transmission wavelength 340–500 nm (Asahi Spectra Co., Ltd.), and a Glan-Taylor prism polarizer was inserted in front of the sample, to produce linearly polarized light (LP-L). The LP-L impinged on the Azo-PAA films at normal incidence. Finally, the photo-aligned film was converted into polyimide by thermal imidization at 250°C for 2 h in a nitrogen atmosphere.

To determine the degree of swelling, the thickness of the Azo-PAA films was determined before and after the ODA vapor treatment by spectroscopic ellipsometry (J. A. Woollam M-2000). The spectroscopic ellipsometry data at different angles of incidence of 55°, 60°, and 65° were simultaneously analyzed. The photo-induced in-plane anisotropy of the Azo-PAA and Azo-PI films were evaluated by measuring the polarized UV-visible (vis) absorption spectra at normal incidence in a transmission geometry. The spectrometer system used in this measurement was described elsewhere [20].

Results and Discussion

First we examined the swelling of Azo-PAA films caused by the ODA vapor treatment. Figure 2 shows the thickness and the refractive index (at wavelength of 700 nm) of the Azo-PAA films exposed to ODA vapor for different treatment times. Although the ODA vapor treatment was carried out at 55°C in the previous study [19], here it was performed at 80°C to shorten the treatment time. The film thickness and the refractive index were obtained by assuming a three-layered structure (air/swollen Azo-PAA/quartz) and analyzing the ellipsometric data in the transparent wavelength region (700 – 1000 nm) with the Cauchy dispersion formula. The film thickness, which was 17.8 ± 0.4 nm before the ODA vapor treatment, increased with increasing ODA vapor treatment time, reaching 50 nm at 1 h, and beyond this treatment time it became almost constant. The inset of Fig. 2 shows the swelling ratio, defined by d/d_0, as a function of the ODA vapor treatment time, where d_0 and d are the film thickness before and after the ODA vapor treatment, respectively. On the

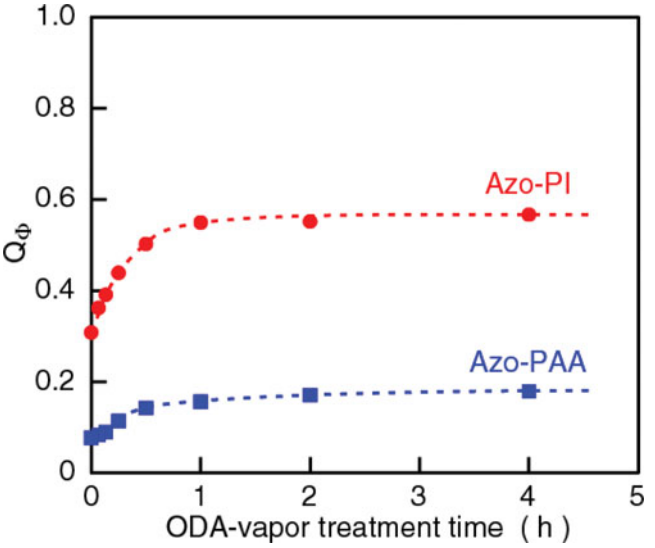

Figure 3. ODA vapor treatment time dependence of the in-plane order parameters Q_Φ of the Azo-PAA(PI) backbone structure, where the data points for Azo-PAA and Azo-PI films are plotted by the filled squares and circles, respectively. For all samples, the ODA vapor treatment was performed at 80°C, and the LP-L exposure in photo-alignment was 39 J/cm^2. The broken curves are guides to the eye.

other hand, the refractive index initially decreased, and it became almost constant in the treatment time range of more than 1 h. Since the refractive index (1.45 at 589 nm at 20°C [21]) of ODA is lower than that (1.843 ± 0.008 at 700 nm) of the as-spin-coated Azo-PAA film, the initial decrease of the refractive index can be understood by the swelling caused by absorbing ODA molecules. These dependences on the ODA vapor treatment time show that the swelling of the Azo-PAA film is almost completed in the first hour, and the swelling ratio is saturated at ∼300%. This saturation behavior suggests that the swelling is promoted by salt formation of polyamic acid and ODA [22]. The swelling is probably limited by the number of carboxylic acid groups in the Azo-PAA film.

Next, we examined the photo-induced in-plane anisotropy of the Azo-PAA and Azo-PI films treated with ODA vapor at 80°C at different treatment times. In this experiment, the ODA-vapor-treated Azo-PAA films were irradiated with LP-L of 39 J/cm^2 at normal incidence. The in-plane anisotropy was determined from the polarization dependence of the absorption band assigned to the π-π^* transition of azobenzene, which is polarized along the backbone structure. (The polarized UV-vis absorption spectra of the Azo-PAA and Azo-PI films treated with and without ODA vapor are shown in Fig. 2 of ref. [19].) The in-plane molecular order parameter Q_Φ defined by $(A_\perp - A_{/\!/})/(A_\perp + A_{/\!/})$ [23,24] was used as a measure of the anisotropic in-plane orientation of the backbone structure, where $A_{/\!/}$ and $A_\perp$, respectively, are the absorbance for the UV-vis light polarized parallel and perpendicular to the polarization direction of the LP-L used in photo-alignment. $Q_\Phi = 1$ means that all backbone structures align perpendicular to the polarization direction of the LP-L, and $Q_\Phi = 0$ means isotropic (random) in-plane molecular orientation. Figure 3 shows the ODA vapor treatment time dependence of the in-plane order parameters ${Q_\Phi}^{PAA(PI)}$ of the Azo-PAA(PI) backbone structure, where the data points for the Azo-PAA and Azo-PI films are plotted by the filled squares and circles, respectively. ${Q_\Phi}^{PI}$ was much larger

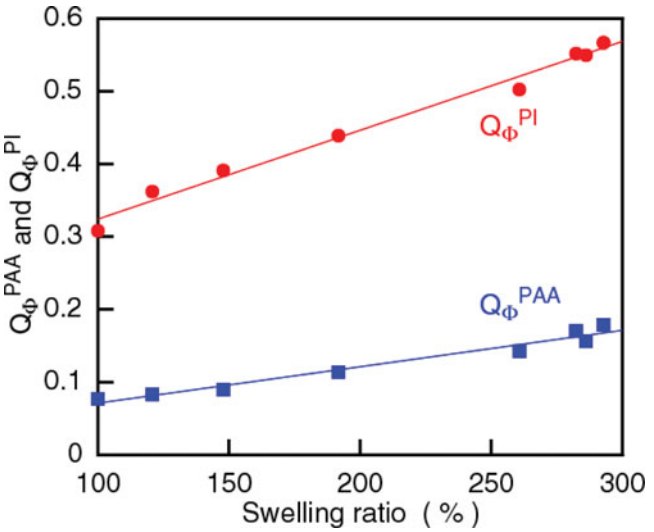

Figure 4. Relation between the photo-induced in-plane anisotropy ($Q_\Phi{}^{PAA}$ and $Q_\Phi{}^{PI}$) and the swelling ratio. The strait solid lines were obtained by the least squares method.

than $Q_\Phi{}^{PAA}$, independent of the ODA vapor treatment time, indicating that the molecular order enhancement occurs during thermal imidization. This is the characteristic nature of the Azo-PAA materials [16]. Both $Q_\Phi{}^{PAA}$ and $Q_\Phi{}^{PI}$ increased with increasing ODA vapor treatment time over the first hour, and then saturated. This behavior is almost the same as the ODA vapor treatment time dependence of the swelling ratio shown in the inset of Fig. 2. To clearly show the correlation, the photo-induced in-plane anisotropy was plotted in Fig. 4 as a function of the swelling ratio. Linear relations were obtained for both $Q_\Phi{}^{PAA}$ and $Q_\Phi{}^{PI}$. This strong positive correlation clearly indicates that the photo-induced rotation efficiency of the Azo-PAA backbone structure increases with increasing swelling ratio. From the saturation behaviors shown in Figs. 2 and 3, the sufficient ODA vapor treatment time at 80°C was found to be 1 h.

Finally, we would like to mention the importance of the process order of alkyl-amine vapor treatment (AV) and photo-alignment (PA). We prepared two Azo-PI photo-alignment layers in different process orders. In this experiment, the ODA vapor treatment was performed at 55°C for 22 h, and the LP-L exposure in photo-alignment was 146 J/cm^2. Figure 5(a) shows the variation of the polarized UV-vis absorbance ($A_\perp$ and $A_{/\!/}$) and the in-plane molecular order parameter (Q_Φ) at each fabrication step for the photo-alignment layer treated with alkyl-amine vapor *prior to* photo-alignment (AV→PA). After the alkyl-amine vapor treatment, the absorbance slightly decreased, indicating the relaxation of the planar orientation of the Azo-PAA backbone structure. This orientation relaxation can be understood easily by the swelling of the Azo-PAA film. Then, the in-plane anisotropy was induced by photo-alignment: $Q_\Phi{}^{PAA}(\text{AV}\rightarrow\text{PA}) = 0.28$, and then it was enhanced by thermal imidization. The in-plane molecular order parameter of the resultant photo-alignment layer was very large: $Q_\Phi{}^{PI}(\text{AV}\rightarrow\text{PA}) = 0.73$. Figure 5(b) shows the data for the photo-alignment layer treated with alkyl-amine vapor *after* photo-alignment (PA→AV). The photo-induced in-plane anisotropy was relatively small: $Q_\Phi{}^{PAA}(\text{PA}) = 0.17$, and furthermore, it reduced after the alkyl-amine vapor treatment: $Q_\Phi{}^{PAA}(\text{PA}\rightarrow\text{AV}) = 0.11$. This result shows that the degree of alignment in the in-plane direction is also relaxed by the alkyl-amine vapor

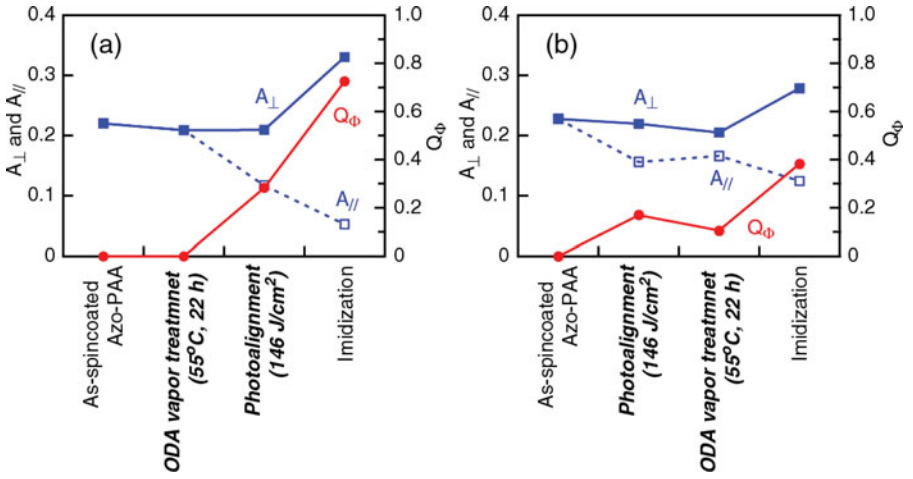

Figure 5. Variation of the polarized UV-vis absorbance ($A_{\perp}$ and $A_{//}$) and the in-plane molecular order parameter (Q_{Φ}) at each fabrication step for the photo-alignment layers prepared in the different process orders: (a) alkyl-amine vapor treatment *prior to* photo-alignment (AV→PA) and (b) alkyl-amine vapor treatment *after* photo-alignment (PA→AV).

treatment. The in-plane molecular order parameter, ${Q_{\Phi}}^{PI}$(PA→AV), of the resultant photo-alignment layer was 0.38, which was much smaller than ${Q_{\Phi}}^{PI}$(AV→PA) and also smaller than that (${Q_{\Phi}}^{PI}$(PA) = 0.45 [19]) of the photo-alignment layer prepared without alkyl-amine vapor treatment: *i.e.,* ${Q_{\Phi}}^{PI}$(AV→PA) >> ${Q_{\Phi}}^{PI}$(PA) > ${Q_{\Phi}}^{PI}$(PA→AV). This relation shows that alkyl-amine vapor treatment must be performed prior to photo-alignment for enhancing the photo-alignment efficiency of the Azo-PI film.

Conclusion

We have investigated the photo-alignment property of the Azo-PAA film swollen by ODA vapor treatment. The thickness of the Azo-PAA film initially increased with increasing ODA vapor treatment time, and then it saturated. The 18 nm-thick Azo-PAA film swelled by ~300% after the ODA vapor treatment at 80°C for 1 h. The photo-induced in-plane anisotropy of the swollen Azo-PAA films increased with increasing swelling ratio. The in-plane anisotropy of the resultant Azo-PI photo-alignment layer also increased with the swelling ratio. We found that the photo-induced in-plane anisotropy is correlated directly with the swelling ratio, not with the ODA vapor treatment time. This means that the photo-alignment efficiency of the Azo-PAA (PI) backbone structure increases with increasing degree of swelling. In addition, we pointed out the importance of the process order of alkyl-amine vapor treatment and photo-alignment. Alkyl-amine vapor treatment must be performed prior to photo-alignment for enhancing the photo-alignment efficiency.

Acknowledgments

We would like to thank N. Tamura of JNC Petrochemical Co. for supplying the polyamic acid solution used in this work.

Funding

A part of this work was supported by JSPS KAKENHI Grant Numbers 21560023 and 25286045.

References

[1] Ogawa, K., Mino, N., & Nakajima, K. (1990). *Jpn. J. Appl. Phys. Part 2*, *29*, L1689.
[2] Chaudhari, P., Lacey, J., Lien, S. -C. A., & Speidell, J. (1998). *Jpn. J. Appl. Phys. Part 2*, *37*, L55.
[3] Chaudhari, P., Lacey, J., Doyle, J., Galligan, E., Lien, S. -C. A., Callegarl, A., Hougham, G., Lang, N. D., Andry, P. S., John, R., Yang, K.-H., Lu, M., Cai, C., Speidell, J., Purushothaman, S., Ritsko, J., Samant, M., Stöhr, J., Nakagawa, Y., Katoh, Y., Saitoh, Y., Sakai, K., Satoh, H., Odahara, S., Nakano, H., Nakadaki, J., & Shiota, Y. (2001). *Nature* (London), *411*, 56.
[4] Gibbons, W. M., Shannon, P. J., Sun, S.-T., & Swetlin, B. J. (1991). *Nature* (London), *351*, 49.
[5] Schadt, M., Schmitt, K., Kozinkov, V., & Chigrinov, V. (1992). *Jpn. J. Appl. Phys. Part 1*, *31*, 2155.
[6] Hasegawa, M. & Taira, Y. (1995) *J. Photopolym. Sci. Technol.*, *8*, 241.
[7] O'Neill, M. & Kelly, S. M. (2000). *J. Phys. D: Appl. Phys.*, *33*, R67.
[8] Kimura, M., Nakata, S., Makita, Y., Matsuki, Y., Kumano, A., Takeuchi, Y., & Yokoyama, H. (2002). *Jpn. J. Appl. Phys.*, *41*, L1345.
[9] Newsome, C. J. & O'Neill, M. (2002). *J. Appl. Phys.*, *92*, 1752.
[10] Chigrinov, V., Muravski, A., Kwok, H. S., Takeda, H., Akiyama, H., & Takatsu, H. (2003). *Phys. Rev. E*, *68*, 061702.
[11] Yaroshchuk, O. & Reznikov, Y. (2012). *J. Mater. Chem.*, *22*, 286.
[12] Schadt, M., Seiberle, H., & Schuster, A. (1996). *Nature*, *381*, 212.
[13] Niitsuma, J., Yoneya, M., & Yokoyama, H. (2008). *Appl. Phys. Lett.*, *92*, 241120.
[14] Park, B., Jung, Y., Choi, H.-H., Hwang, H. -K., Kim, Y., Lee, S., Jang, S. -H., Kakimoto, M. -A., & Takezoe, H. (1998). *Jpn. J. Appl. Phys.*, *37*, 5663.
[15] Usami, K., Sakamoto, K., Uehara, Y., & Ushioda, S. (2005). *Jpn. J. Appl. Phys.*, *44*, 6703.
[16] Sakamoto, K., Usami, K., Kikegawa, M., & Ushioda, S. (2003). *J. Appl. Phys.*, *93*, 1039.
[17] Sakamoto, K., Usami, K., & Ushioda, S., Japan Patent 4620438 (26 January 2011) [in Japanese].
[18] Faetti, S., Sakamoto, K., & Usami, K. (2007). *Phys. Rev. E*, *75*, 051704.
[19] Sakamoto, K., Usami, K., & Miki, K. (2014). *Appl. Phys. Express 7*, 081701.
[20] Sakamoto, K., Usami, K., & Ushioda, S. (2006). *Colloids Surf. A: Physicochem. Eng. Aspects*, 284–285, 635.
[21] Lide, D. R. (Eds.) (1995). *CRC Handbook of Chemistry and Physics* 76th ed., CRC Press Inc.: Florida, USA.
[22] Clayden, J., Greeves, N., & Warren, S. (2012). *Organic Chemistry,* 2nd Edition, Oxford: New York, 207.
[23] Kaito, A., Nakayama, K., & Kanetsuna, H. (1987). *J. Macromol. Sci. Phys. B*, *26*, 281.
[24] Barmentlo, Van Aerle, M., N. A. J. M., Hollering, R. W. J., & Damen, J. P. (1992). *J. Appl. Phys.*, *71*, 4799.